Amyloid
The Journal of Protein Folding Disorders
http://informahealthcare.com/amy
ISSN: 1350-6129 (print), 1744-2818 (electronic)
Amyloid, 2016; 23(3): 168–177
 DOI: 10.1080/13506129.2016.1205974
Taylor & Francis
Taylor & Francis Group

ORIGINAL ARTICLE

2A4 binds soluble and insoluble light chain aggregates from AL amyloidosis patients and promotes clearance of amyloid deposits by phagocytosis†

Mark Renz*, Ronald Torres*, Philip J. Dolan, Stephen J. Tam, Jose R. Tapia, Lauri Li, Joshua R. Salmans, Robin M. Barbour, Paul J. Shughrue, Tarlochan Nijjar, Dale Schenk, Gene G. Kinney, and Wagner Zago

Prothena Biosciences Inc, South San Francisco, CA, USA

Abstract

Amyloid light chain (AL) amyloidosis is characterized by misfolded light chain (LC) (amyloid) deposition in various peripheral organs, leading to progressive dysfunction and death. There are no regulatory agency–approved treatments for AL amyloidosis, and none of the available standard of care approaches directly targets the LC protein that constitutes the amyloid. NEOD001, currently in late-stage clinical trials, is a conformation-specific, anti-LC antibody designed to specifically target misfolded LC aggregates and promote phagocytic clearance of AL amyloid deposits. The present study demonstrated that the monoclonal antibody 2A4, the murine form of NEOD001, binds to patient-derived soluble and insoluble LC aggregates and induces phagocytic clearance of AL amyloid *in vitro*. 2A4 specifically labeled all 21 fresh-frozen organ samples studied, which were derived from 10 patients representing both κ and λ LC amyloidosis subtypes. 2A4 immunoreactivity largely overlapped with thioflavin T–positive labeling, and 2A4 bound both soluble and insoluble LC aggregates extracted from patient tissue. Finally, 2A4 induced macrophage engagement and phagocytic clearance of AL amyloid deposits *in vitro*. These findings provide further evidence that 2A4/NEOD001 can effectively clear and remove human AL-amyloid from tissue and further support the rationale for the evaluation of NEOD001 in patients with AL amyloidosis.

Abbreviations: 2A4, murine homolog of NEOD001; AL amyloidosis, amyloid light chain amyloidosis; ATTR, transthyretin amyloid protein; CPHPC, *R*-1-[6-[*R*-2-carboxypyrrolidin-1-yl]-6-oxo-hexanol] pyrrolindine-2-carboxylic acid; Fc, crystallizable fragment; FLC, free light chain; IHC, immunohistochemistry; LC, light chain; LCM-MS, laser capture microdissection–mass spectrometry; NEOD001, anti–light chain antibody derived from 2A4; PBS, phosphate-buffered saline; TBST, Tris-buffered saline with Tween-20; ThioT, thioflavin T

Keywords

Antibody, cardiac, cryptotope, immunotherapy, macrophage

History

Received 4 March 2016
Revised 18 May 2016
Accepted 22 June 2016
Published online 2 August 2016

Introduction

Systemic amyloidoses are a group of rare disorders characterized by abnormal protein folding and deposition in organs, resulting in organ dysfunction and, in some cases, death. Amyloid light chain (AL) amyloidosis, a fatal disease, is the most common form of systemic amyloidosis [1], affecting an estimated 8 to 14.4 per million persons per year [2–4]. The involved amyloidogenic protein is a misfolded light chain (LC) or LC fragment, produced by clonal plasma cells [5]. Multiple organs and systems can be involved in AL amyloidosis, most commonly the heart (~70% of patients), the kidneys (70% of patients), or both [6–8]. Occasionally, soft tissue, the liver, the gastrointestinal tract and the peripheral and autonomic nervous systems (<20% patients each) are also affected [6–8]. Accumulation of AL often leads to organ failure [8]. In addition, soluble aggregates or precursor aggregates may be directly cytotoxic [9–14]. In the heart, LC-soluble monomers and aggregates may elicit oxidative damage and induce p38 mitogen-activated protein kinase signaling, which can impair excitation–contraction coupling [9,13,14]. LC fibrils in solution can bind to the cardiomyocyte plasma membrane and induce metabolic dysfunction [11,12].

No therapy for AL amyloidosis has yet received regulatory approval. Current treatment options include high-dose

†Portions of the data from this study were presented in poster form at the 57th American Society of Hematology (ASH) Annual Meeting; 5–8 December 2015; Orlando, Florida.

*These authors contributed equally to this work.

Address for correspondence: Wagner Zago, PhD, Prothena Biosciences Inc, 650 Gateway Boulevard, South San Francisco, CA 94080, USA. Tel: +1-650-615-2108. E-mail: wagner.zago@prothena.com

chemotherapy with autologous stem cell transplantation, alkylating agents, steroids, proteasome inhibitors and immunomodulatory drugs [7]. These treatments are intended to reduce the production of immunoglobulin LC precursor proteins by targeting plasma cells, and they often do so successfully. In patients who do experience reduced levels of circulating free light chain (FLC), the probability is increased that they will also experience partial organ improvement, though the likelihood that a hematologic response will result in organ benefit is variable and low. Therefore, a critical unmet need remains for AL amyloidosis therapy that directly and specifically targets misfolded forms of LC to promote the clearance of amyloid deposits, neutralize soluble toxic species, and potentially improve organ function and survival.

NEOD001 is a monoclonal antibody derived from the murine monoclonal antibody 2A4. Both NEOD001 and 2A4 bind a cryptic LC epitope unique to the misfolded protein thought to be exposed during misfolding and aggregation. This cryptotope is likely inaccessible for antibody binding in the native conformation of the FLC or in fully formed immunoglobulin [15]. Accordingly, 2A4 was previously shown to immunoreact with insoluble LC aggregates extracted from AL amyloidosis patient samples while sparing normally folded LC [15]. *In vivo*, 2A4 promoted the clearance of AL amyloid extracts in a mouse amyloidoma model, likely by engaging phagocytes to clear deposits [15].

Herein, we assessed the binding and biological properties of 2A4 by further characterizing its binding specificity to a variety of organs derived from patients with AL amyloidosis using immunohistochemical and biochemical assays, including a newly developed immunoassay specific for aggregated LC. The *in vitro* capacity of 2A4 to opsonize LC aggregates originating from patients' organs and to promote clearance by phagocytes was also assessed. Results of these studies demonstrated that 2A4 specifically binds to both soluble and insoluble LC aggregates and promotes the clearance of insoluble aggregates by macrophage phagocytosis. As such, NEOD001, derived from 2A4, has the potential to restore organ function by directly targeting amyloid deposits, the underlying cause of organ dysfunction in patients with AL amyloidosis.

Methods

Expression, purification and preparation of aggregated LC proteins and antibodies

Human-derived cell lines that express and secrete amyloidogenic λ LC, ALMC-1, and ALMC-2, obtained from the Mayo Clinic (Rochester, MN), were grown as described by Arendt et al. [16], and conditioned media were harvested for protein purification. For recombinant λ LC protein expression, the amino acid sequence of ALMC-1/2 published by Arendt et al. [16] was reverse translated, codon optimized and modified to incorporate flanking restriction sites. The resultant nucleotide sequence was used for *de novo* DNA synthesis. After restriction digestion, the synthesized DNA fragment was cloned into an expression vector to derive the protein expression under the control of a cytomegalovirus promoter. Purified plasmid DNA was transfected into a Chinese hamster ovary cell suspension using Lipofectamine 2000 (Thermo Fisher Scientific, Waltham, MA). Transfected cells were cultured in shake flasks at 37 °C and 7% CO_2, and stable pools were selected using puromycin. For protein production, conditioned media from stable cell pools were harvested after 48 to 72 h. For purification of ALMC proteins, intact immunoglobulin G (IgG) introduced into the growth media was pre-cleared using protein G chromatography (GE Healthcare Life Sciences, Pittsburgh, PA). Affinity chromatography (Lambda FabSelect; GE Healthcare Life Sciences) was used to purify λ FLC from cleared media, with resultant fractions dialyzed into phosphate-buffered saline (PBS; pH 7.4). Purity, monomeric nature and identity of final products were confirmed by sodium dodecyl sulfate–polyacrylamide gel electrophoresis, size exclusion chromatography–high-performance liquid chromatography, and mass spectrometry, respectively.

ALMC λ LC (1 mL protein in PBS; 1 mg/mL) was incubated in a 15-mL conical tube that was shaken at 500 rpm at a temperature of 57 °C for 5 days to induce aggregation. Aggregation was monitored over time using thioflavin T (ThioT) fluorescence. Briefly, a 10-μL sample was added to 140 μL ThioT read buffer (25 μM ThioT, 100 mM glycine, pH 8.5), and fluorescence was determined at 450/482 $\lambda_{ex/em}$. Aggregation was confirmed by transmission electron microscopy and atomic force microscopy. The generation of monoclonal antibody 2A4 was previously described [15].

Histology and image analysis

Tissue samples

Fresh-frozen tissue samples were generously donated by Merrill Benson (Indiana University School of Medicine, Indianapolis, IN) and Michaela Liedtke (Stanford University, Palo Alto, CA) and were purchased from the National Disease Research Interchange (Philadelphia, PA). Fresh-frozen normal tissue was obtained from BioreclamationIVT (Baltimore, MD), and positive controls were purchased from American MasterTech (Lodi, CA). Fresh frozen samples were embedded without fixation in OCT media and were serially cryosectioned (10 μm) and stored at –80 °C.

Amyloid labeling

Amyloid was detected using both ThioT and alkaline Congo red (Puchtler's modified protocol) [17] stains, and tissue labeling was examined in subsequent immunohistochemical assays.

Amyloid typing

Amyloid typing was performed by immunohistochemistry and by laser capture microdissection–mass spectrometry (LCM-MS). A panel of eight commercial anti-LC polyclonal antibodies directed against either total LC or FLCs was used for immunohistochemistry. Rabbit polyclonal antibodies to human λ LC (1:150 000), κ LC (1:150 000), λ FLC (1:60 000), and κ FLC (1:20 000) were purchased from Dako (Carpinteria, CA). Sheep polyclonal antibodies to human λ LC (1:5000), κ LC (1:5000), λ FLC (1:150 000), and κ FLC (1:150 000) were supplied by The Binding Site (Birmingham, UK). Rabbit antibody anti-serum amyloid-P (1:500) was purchased from Novus Biologicals (Littleton, CO). Tissue

was screened for non-LC (AL) amyloid deposits using a mouse monoclonal antibody to human amyloid A (AA; 10 μg/mL, Dako) and a rabbit polyclonal antibody to human transthyretin amyloid protein (ATTR; 1:5000, Dako). Amyloid typing on paraffin-embedded tissue was performed at the Mayo Clinical Laboratory (Rochester, MN) using a validated LCM-MS protocol [18,19].

2A4 immunohistochemistry

All tissue was stained on a Bond Rx (Leica Biosystems, Buffalo Grove, IL) automated stainer using a proprietary Bond Polymer Refine Detection kit (DS980; Leica Biosystems) or a Bond Research kit (DS9455; Leica Biosystems). Before immunoperoxidase labeling, endogenous peroxidases were quenched using the glucose oxidase method (1 h, 37 °C), and tissue was subsequently incubated with 2A4 (10 μg/mL, 5% [vol/vol] normal goat serum in 0.25% [vol/vol] Triton X-100 in 1 × PBS, 1 h) and with antimouse and antirabbit horseradish peroxidase polymeric secondary antibody cocktail (8 min) and was visualized with DAB chromogen (brown precipitate).

Serial indirect double-immunofluorescence was performed to demonstrate colocalization of 2A4 with λ and κ FLCs. Tissue slides were first incubated with 2A4 (10 μg/mL, 1 h), followed by detection with an Alexa Fluor 488–conjugated goat antimouse secondary antibody (1:250 for 1 h; Invitrogen, Carlsbad, CA). This was followed by 1-h incubation with λ FLC (1:500) or κ FLC (1:500) (Dako) and was detected with an Alexa Fluor 647 goat antirabbit secondary antibody (Invitrogen).

To verify labeling specificity, immunolabeling in specimens with confirmed AL amyloidosis (positive controls) was compared with that in matched organ/tissue from patients without amyloidosis or from patients with ATTR amyloidosis (negative controls). Adjacent slides were immunolabeled with non-immune isotype primary antibodies (control IgGs) or by omitting the primary antibodies altogether in the standard labeling procedure to control for antibody specificity. Specificity of 2A4 to aggregated LC was confirmed by preabsorbing 2A4 with a 10-fold molar excess of aggregated ALMC-2 or monomeric LC *in vitro*. The preabsorbed antibody-protein solution was then applied to tissue laden with LC pathology, and the 2A4 immunohistochemistry procedure was carried out as outlined. The sensitivity of 2A4 antigens to aldehyde cross-linking was assessed by fixing the AL tissue in 10% neutral-buffered formalin from 1 min to 48 h before 2A4 immunohistochemical labeling.

Image analysis

Amyloid burden was categorized based on the percentage area of tissue positive for deposits labeled by ThioT, Congo red, λ and κ FLC and 2A4 immunoreactivity. Labeling was ranked semiquantitatively as (–) no detectable immunoreactivity or as (+) 10–25%, (++) 26–50%, and (+++) >50% of the total tissue area stained.

Tissue was classified as containing AL amyloid if it exhibited specific staining for any of the LC antibodies. The predominantly affected LC subtype was determined by the intensity of λ and κ FLC immunoreactivity and confirmed by LCM-MS when sufficient material was available. The sample was classified as non-AL amyloidosis if amyloid deposits were strongly and uniformly transthyretin or amyloid A immunoreactive.

ThioT labeling was evaluated with a BX61 microscope (Olympus, Center Valley, PA) equipped with a 10×/0.40 and an UPlanSApo 20×/0.75 objective (Olympus) using appropriate fluorescence filters. Congo red–stained slides were evaluated between a crossed-polarizer and an analyzer to view the characteristic green birefringence of amyloid deposits. Images were acquired with a Retiga EXi digital camera (QImaging, Surrey, BC, Canada) and were imported with the MetaMorph imaging system (version 7.6.4.0; Molecular Devices, Sunnyvale, CA). Whole slides were digitally imaged with a NanoZoomer 2.0HT slide scanner (Hamamatsu, Bridgewater, NJ) fitted with UPlanSApo 20×/0.75 objective (Olympus).

Immunoassay for measuring aggregated LC

Tissue extraction and insoluble fraction preparation

All tissue extraction procedures were carried out at 4 °C using a protocol modified from Cohen and Calkins [20]. Briefly, approximately 10 g of each amyloid-laden tissue was homogenized in 25 mL of 0.15 M NaCl in H_2O in a VDI 12 (VWR) high-speed homogenizer (5 min). The homogenate was then centrifuged (10 000*g*; 30 min), the supernatant was discarded, and the sediment was re-homogenized as described with 25 mL of 0.15 M NaCl and centrifuged (10 000*g*; 30 min). These steps were repeated 6 to 7 times. The final insoluble material was resuspended in a final volume of 10 mL PBS. The content of each crude extract is expressed as 1 mL/g starting material. Tissue extraction was based on tissue mass and was performed in physiological solution and in the absence of detergents to preserve the native state of the proteins. The amyloid nature of the extracts was confirmed by immunostaining experiments demonstrating the presence of SAP and ThioT.

Soluble fraction preparation

Preparation of the soluble fraction was performed as described for the insoluble fraction except that the tissue was homogenized once and centrifuged (10 000*g*; 30 min) to pellet any insoluble material. The supernatant from this step was then centrifuged (100 000*g*; 1 h; 4 °C). The supernatant and the pellet from this step were harvested and referred to as the soluble and the insoluble aggregate extracts, respectively.

MSD electrochemiluminescence assay for aggregated LC

A standard 96-well, single-spot MSD plate (Meso Scale Discovery, Rockville, MD) was coated with the capture antibody (2A4) overnight at 4 °C. The plate was then blocked (3% MSD Blocker A; 1 h) on a shaking platform (450 rpm) and was washed thrice with Tris-buffered saline with Tween-20 (TBST). Samples, tissue extracts and recombinant LC aggregates were added to wells and incubated (2 h; room temperature) with constant shaking. All samples were diluted with 1 × sample diluent (1.5 mM sodium phosphate [monobasic], 8 mM sodium phosphate [dibasic], 145 mM NaCl, 0.6% BSA, 0.05% Triton X-405), and plates were rewashed thrice with TBST.

Biotinylated 2A4 was used as reporter antibody and was added to each well and incubated at a final concentration of 2 μg/mL (1 h; room temperature) with shaking. After incubation, plates were washed thrice with TBST, and SULFO-TAG Streptavidin (R32AD-5; Meso Scale Discovery) was added at a final concentration of 1 μg/mL and incubated (1 h) with shaking. After a final wash and inversion with patting on towels to blot dry, 1 × read buffer (Read Buffer T with Surfactant, R92TC-1; Meso Scale Discovery) was added to each well, and the plate was read using the standard detection parameters on the Meso Sector S600 (model 1201; Meso Scale Discovery) plate reader. Analysis was performed on MSD Discovery Workbench Software (version 4.0.12.1; Meso Scale Discovery). Relative levels of LC aggregates in soluble and insoluble fractions were measured as electrochemiluminescence signal.

Size exclusion chromatography

Soluble 100 000*g* supernatants were resolved using a Superdex 200 10/300 size exclusion chromatography column (GE Healthcare Life Sciences). The column was loaded with 0.5 mL supernatant and was resolved at a flow rate of 0.2 mL/min. Fractions were collected throughout the elution period and assayed for 2A4 reactivity using the MSD aggregated LC assay described above.

Phagocytosis

AL amyloidosis organ extracts

In vitro phagocytosis assays were performed with insoluble fractions of an AL amyloidosis heart extract or expressed and aggregated recombinant ALMC LC either neat or pre-labeled with the pH-sensitive dye pHrodo Red (Thermo Scientific, Waltham, MA) by amine coupling. The sample (1 mg/mL) was incubated in pHrodo dye for 15 min at 37 °C using a protein/dye ratio of approximately 15:4 according to the manufacturer's specifications. Excess pHrodo label was removed by diafiltration in a spin concentrator with a 10K molecular weight cutoff (Thermo Scientific Pierce, Waltham, MA), and the pHrodo-labeled particles were resuspended in 1 × PBS and were used immediately.

Phagocytosis assay

THP-1 human monocytes (ATCC, Manassas, VA) were cultured in RPMI with 10% low IgG serum + penicillin/streptomycin. To assess the clearance of extracellular deposits, a 20-μg/mL aliquot of AL amyloidosis heart extract was incubated on collagen-coated well plates for 30 min and washed extensively with PBS to remove any unbound material. THP-1 cells were incubated in the presence of 40 μg/mL of either 2A4 or an isotype control antibody at 37 °C in cell culture media for 24 h. Cells were then washed, fixed in PFA, and immunolabeled to detect λ FLC (1:500). The area of the specific labeling was calculated. Importantly, 2A4 and the λ FLC antibodies recognize distinct epitopes in the unfolded LC and do not compete for LC binding (not shown). Thus, any reduction of signal is interpreted as clearance of the LC deposit and not as 2A4-mediated interference of FLC antibody signal detection. For the assessment of LC internalization, a 20-μg/mL aliquot of pHrodo-labeled AL amyloidosis heart extract or recombinant, insoluble ALMC aggregates were separately pre-incubated with 40 μg/mL 2A4 or an isotype control antibody at 37 °C in cell culture media for 30 min before the addition of THP-1 cells in suspension. After incubation (3 h), cells were washed thrice with cell culture media, incubated in the same media for 10 min, and washed twice with FACS buffer (1% fetal bovine serum in PBS). Red pHrodo fluorescence intensity was detected using standard flow cytometry methods (FACSAria II; BD Biosciences, Franklin Lakes, NJ). Mean fluorescence intensity was calculated from the average fluorescence of each cell.

Epifluorescence microscopy was carried out in a similar fashion. Briefly, remaining cells were transferred to glass chamber slides and imaged by inverted microscopy using an IX81 inverted microscope (Olympus). For time-lapse analysis, the sample was analyzed immediately after the exposure of LC aggregates to cells and the antibody, and images were acquired every 3 min using an IX81 inverted microscope (Olympus) equipped with a Bold Line temperature and humidity-controlled stage-top chamber (Oko Labs, Burlingame, CA) set at 25 °C with 5% CO_2 at a flow rate of 0.3 L/min and 85% relative humidity.

Statistical analysis

Results are presented as mean ± standard error. Differences between 2A4 and IgG control groups were examined by 2-tailed Student *t* tests. A criterion for statistical confidence of $p < 0.05$ was adopted.

Results

NEOD001 binds to soluble and insoluble LC aggregates

We demonstrated previously that 2A4 bound to synthetic, insoluble amyloid fibrils composed of highly amyloidogenic recombinant Wil and Jto λ6 LC variable (rVλ6) domains and to insoluble human AL amyloid deposits extracted from AL amyloidosis tissue [15]. Here we explored whether 2A4 bound to soluble aggregates more representative of the intermediate states of misfolding and aggregation of LC in patients. We used a full-length λ FLC that is naturally secreted *in vitro* from human ALMC cells—a cell line derived from a patient with cardiac AL amyloidosis [16]. This LC forms a heterogeneous population of secreted soluble LC aggregates over time, allowing the opportunity to investigate the ability of 2A4 to bind to various species.

Aggregation of purified ALMC samples was elicited by constant agitation at the established melting temperature [16] and resulted in a mixed population of predominantly LC globules (approximately 20–40 nm in diameter) and short LC fibrils (approximately 100 nm in length) (Figure 1A and B). The presence of short fibrils was also evident by transmission electron microscopy (Supplementary Figure S1). Size exclusion chromatography fractionation of soluble ALMC LC revealed several distinct populations of small intermediates, consistent with the presence of a diverse LC population (Supplementary Figure S2).

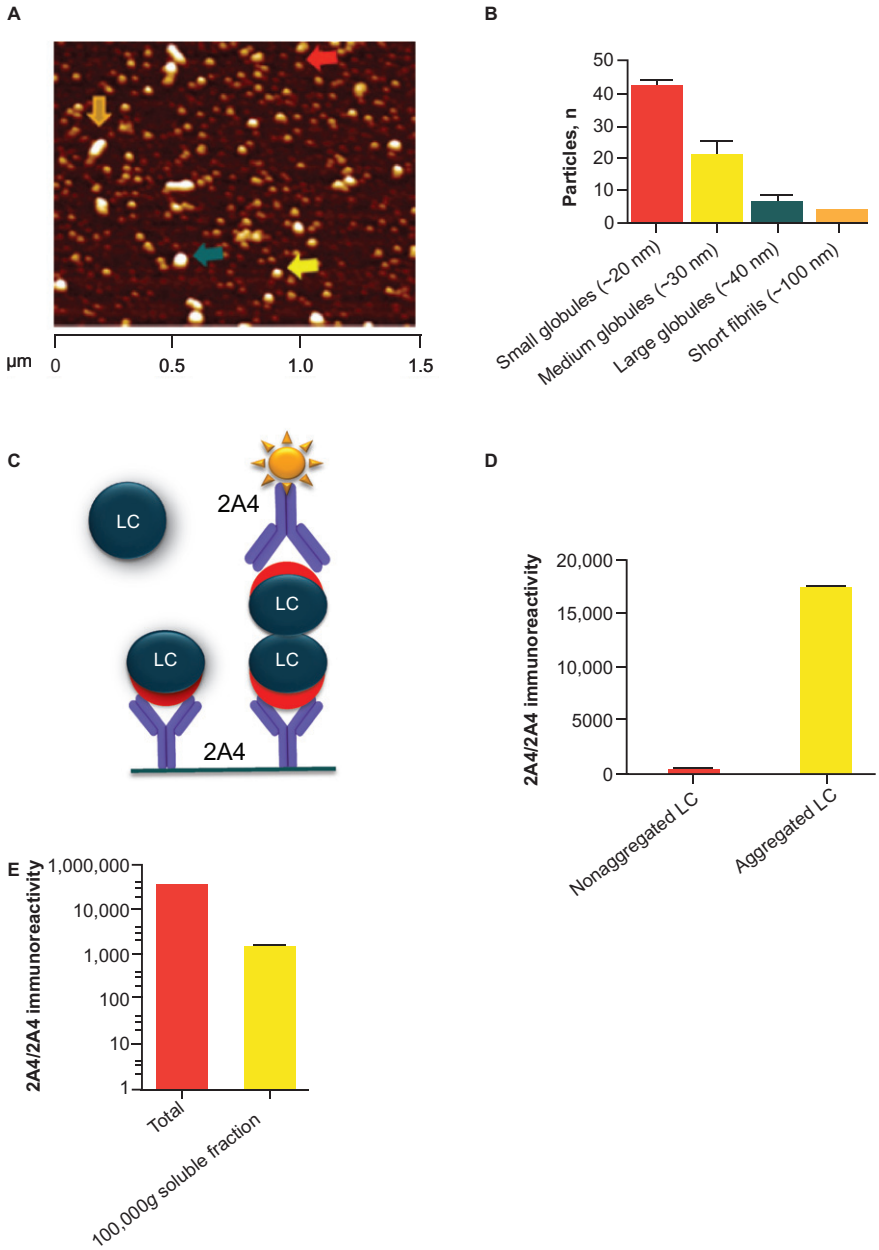

Figure 1. 2A4 bound to soluble and insoluble LC aggregates from ALMC cells. (A, B) Particles in the soluble LC fraction were analyzed using atomic force microscopy. Small (red arrow), medium (yellow arrow) and large (green arrow) globules are present, alongside apparent short fibrils (orange arrow). (C) Principle of the sandwich MSD electrochemiluminescence assay developed to detect LC aggregates. (D) 2A4 specifically binds ALMC protein that is aggregated. (E) After fractionation by centrifugation, both soluble and insoluble fractions exhibited strong 2A4 reactivity. Values represent the mean ± SEM of results from three optical fields (B) or three experimental replicates (D, E).

To assess 2A4 binding to ALMC LC aggregates, we developed a sandwich immunoassay based on the MSD electrochemiluminescence platform (Meso Scale Discovery), which captured misfolded LC with 2A4 and detected it with biotinylated 2A4 (Figure 1C). Only LC aggregates with at least two binding sites per molecule can be both captured and detected with this approach, thus allowing discrimination between aggregated and monomeric LC. Accordingly, before aggregation, the crude ALMC LC extract showed no specific signal (Figure 1D). After aggregation, however, a strong signal was detected (Figure 1D), confirming previous observations with recombinant LC fragments [15]. After fractionation, both soluble and insoluble ALMC LC fractions exhibited strong 2A4 reactivity (Figure 1E), indicating that the cryptotope to which 2A4 binds becomes exposed during the early stages of LC misfolding and aggregation.

NEOD001 binds to both soluble and insoluble aggregates extracted from patients' tissue

We used the MSD sandwich immunoassay (Meso Scale Discovery) on fresh frozen organ extracts from patients with AL amyloidosis to determine whether intermediate species, as observed in ALMC LC aggregates, were also detectable in soluble fractions from patients' tissue.

Strong 2A4 immunoreactivity was detected in organ homogenates of 19 of 20 organ samples studied from 10 patients with AL amyloidosis, representing both λ- and κ-predominant LC deposits with variable amounts of

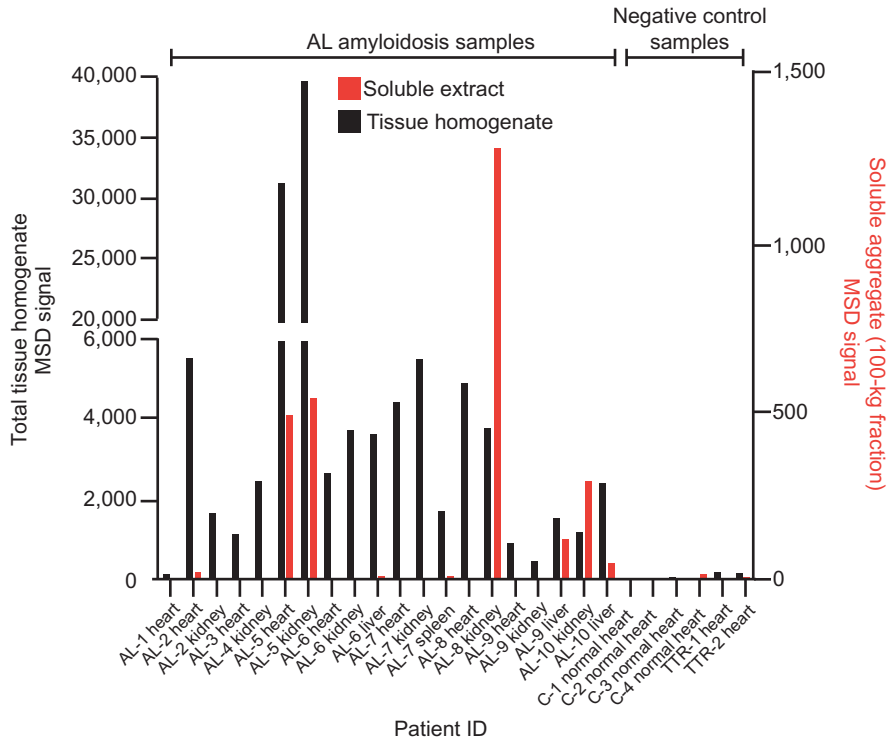

Figure 2. 2A4 binds to both soluble and insoluble aggregates in various organs of patients with AL amyloidosis. Fresh-frozen samples from 10 patients (representing both λ and κ LC amyloid) were assessed using the MSD electrochemiluminescence assay. Strong reactivity to 2A4 was observed in 19 of 20 crude fractions and 6 of 19 soluble fractions studied. Values represent the relative levels of LC aggregates measured as electrochemiluminescence signal.

Table 1. Summary of 2A4 immunoreactivity to AL amyloidosis patient tissue.

Patient ID	Predominant involved FLC (LCM-MS)	Predominant involved FLC (IHC)	Organ	Thioflavin-T content	2A4 IHC (rating)
AL-1	ND	λ	Heart	+++	+++
AL-2	λ	λ/κ	Heart	++	+
			Kidney	+	++
AL-3	κ	κ	Heart	+	+
AL-4	κ	κ	Kidney	+++	+++
AL-5	λ	λ	Heart	+++	++
			Kidney	+++	+++
AL-6	λ	λ/κ	Heart	++	++
			Kidney	+++	+++
			Liver	+++	+++
AL-7	Indeterminate	λ	Heart	+	++
			Kidney	++	++
			Spleen	+	++
AL-8	λ	λ	Heart	++	++
			Kidney	–	++
AL-9	Indeterminate (CR^-)	κ	Heart	+	+
			Kidney	++	++
			Liver	+	++
AL-10	λ	λ/κ	Heart	++	+
			Kidney	++	+
			Liver	+++	+++

CR^-, Congo red negative; FLC, free light chain; IHC, immunohistochemistry; LCM-MS, laser capture microdissection–mass spectrometry; ND, not determined; —, not detected.

deposition (Figure 2). The broad variability in absolute signal levels between specimens likely reflected the different extent, and regional variability, of amyloid deposition observed among samples, which was generally confirmed by immunohistochemistry (Table 1). No specific signal was observed in organs from healthy controls or organs containing ATTR deposits, further corroborating the specificity of the antibody for LC amyloid.

2A4 immunoreactivity was also detected in the soluble fraction of a subset of samples (6 of 19 organs studied) (Figure 2). Interestingly, the relative levels of immunoreactivity in the soluble fractions did not consistently correlate with matched insoluble fractions under the conditions tested, which might suggest that soluble and insoluble aggregates can be formed by distinct pathways or that factors related to the LC sequence or tissue microenvironment determine the

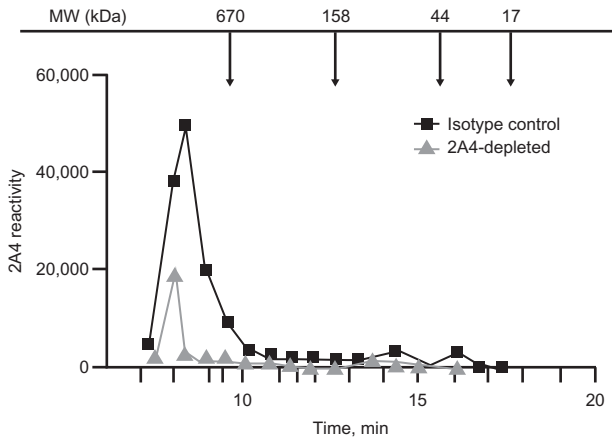

Figure 3. Size exclusion chromatography and 2A4 reactivity to soluble LC aggregates extracted from the heart of a patient with AL amyloidosis. A wide range of soluble LC aggregates can be immunodepleted by 2A4. Values represent electrochemiluminescence signal.

relative equilibrium between soluble aggregates and mature fibrils. These results support the concept that 2A4 binds to soluble aggregates that might be present in the vicinity of amyloid deposits in AL organs.

To better characterize the relative mass of soluble 2A4-reactive species and to assess binding specificity, we performed size exclusion chromatography fractionation of an AL amyloidosis heart-soluble extract after immunoprecipitation with 2A4-coated or isotype IgG control–coated beads. Using the MSD sandwich immunoassay (Meso Scale Discovery) as a detection platform, 2A4-reactive species with molecular weights higher than 650 kDa were eluted in the isotype control group (Figure 3). These species were substantially reduced by 2A4 immunoprecipitation, further supporting binding specificity of the antibody.

2A4 immunoreactivity identifies LC amyloid deposits in patients' tissue

The results above and the data from a previous report [15] have demonstrated that 2A4 avidly and specifically binds to aggregated LC extracted from AL patient organs. However, 2A4 was previously shown to immunohistochemically label patient amyloid tissue samples to a variable extent after formalin fixation and paraffin processing [15]. We were curious to know whether this variability was attributable to the fixation process, which may change the presentation of the necessary cryptic epitope that 2A4/NEOD001 target [21]. Accordingly, we evaluated the ability of 2A4 to bind to fresh-frozen sections isolated from patients with AL amyloidosis (or relevant control samples). 2A4 immunohistochemical analysis was performed on 21 fresh-frozen (unfixed) AL amyloidosis organ samples (heart, kidney, liver and spleen) from 10 patients with AL amyloidosis representing both λ and κ amyloidosis subtypes (Figure 4, Table 1). The presence and extent of amyloid in this tissue were confirmed by Congo red and ThioT staining (Figure 4B and E, Table 1, and Supplementary Figure S3). Because the archival samples did not have accompanying clinical histories, we subtyped the putative involved LC (λ or κ) using immunohistochemistry with specific λ or κ antibodies (Figure 4H and K, Table 1). LCM-MS was also used for amyloid and LC subtyping in a subset of samples (9 of 10 patients) and largely demonstrated concordance with histologic subtyping (Table 1). Interestingly, although most organs showed a predominance of either λ or κ LC immunoreactivity, 3 of 10 patients showed comparable extents of fibrillar light chains of both subtypes in their affected organs (referred to as λ/κ in Table 1). As expected because of its ubiquitous presence in amyloid deposits [22], serum amyloid-P protein (SAP) was detected by LCM-MS in all the samples tested.

Every unfixed AL amyloidosis tissue sample assessed in the present study showed specific 2A4 immunoreactivity, localized to extracellular deposits (Figure 4A, D, G, J, and M, Table 1). Although the areas immunolabeled by 2A4 largely overlapped with ThioT (Figure 4A, B, D, and E) and Congo red (Supplementary Figure S3), additional 2A4-positive areas were negative for the amyloid dyes and likely represented amorphous LC deposits. 2A4 immunoreactivity colocalized with both λ and κ FLC (Figure 4G–L). The specificity of 2A4 and anti-λ or -κ FLC immunolabeling was confirmed by the lack of staining of tissue from patients with ATTR amyloidosis or from healthy subjects.

To confirm that the fixation process might have contributed to the variability observed in a previous study [15], we next assessed whether aldehyde fixation compromised 2A4 binding to AL amyloid from patient samples by exposing fresh-frozen (unfixed) AL tissue to controlled post-fixation intervals in formalin (1 min to 48 h). We observed that fixation rapidly (1 min) and substantially suppressed 2A4 immunoreactivity (Figure 4M–O), whereas ThioT staining was unaffected, even after 24 h of fixation. Therefore, the variability in the specific 2A4 signal reported in a previous study [15] likely relates to an artifact of tissue fixation and the resultant loss of the relevant 2A4 epitope.

These results, together with the biochemical results, indicate that 2A4 binds to both λ and κ LC amyloid deposits and that the 2A4 cryptotope is sensitive to chemical modifications of the aggregated LC by aldehyde fixatives.

2A4 promotes phagocytosis of AL amyloidosis aggregates *in vitro*

Previously, we reported that immunotherapy with 2A4 reduced the mass of amyloid deposits in mice bearing human AL amyloidomas extracted from patients with AL amyloidosis [15]. Notably, macrophages were observed in the vicinity of and within amyloid deposits in 2A4-treated mice, suggestive of phagocytic clearance. Here we explored whether 2A4 could directly induce amyloid phagocytosis in an *in vitro* experimental setting.

Insoluble LC amyloid–containing fractions from heart extracts of patients with AL amyloidosis were incubated with human monocyte THP-1 cells in the presence of 2A4 or an IgG control. Immunostaining experiments demonstrated that the tissue extracts were ThioT and SAP positive, confirming their amyloid nature [22]. The area of extracellular deposits, identified by immunostaining for λ LC, was significantly reduced by 2A4 incubation ($p < 0.0001$) compared with the IgG control antibody incubation (Figure 5A). By using either AL tissue extracts (Figure 5B and C) or insoluble,

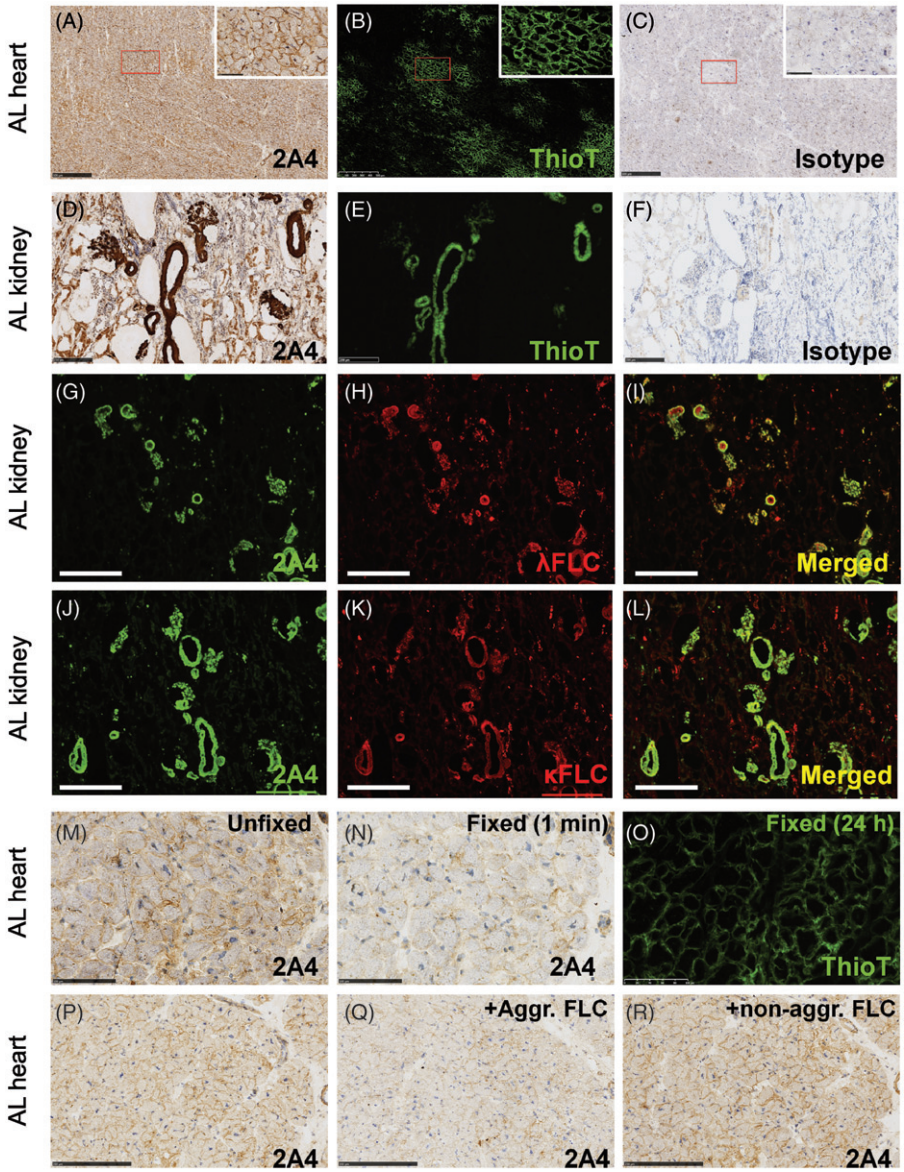

Figure 4. 2A4 specifically immunolabels cardiac and renal λ and κ FLC deposits from patients with light chain (AL) amyloidosis. (A–C) Cardiac 2A4 immunolabeling appears diffusely pericellular, intercalating the fibers of the myocardium. Immunoreactivity overlaps predominantly with ThioT labeling, but amorphous deposits (ThioT-negative) also co-label with the antibody. (D–F) 2A4 strongly decorated the glomeruli and renal vasculature and co-localized with λ and κ FLC deposits (G–L). (M–O) 2A4 immunoreactivity was reduced in fresh-frozen cardiac samples after brief (1 min) post-fixation with formalin, whereas ThioT staining was unaffected. (P-R) 2A4 preabsorptions with aggregated LC proteins, but not monomeric LC, attenuated 2A4 immunoreactivity in cardiac tissue. +Aggr. FLC, aggregated free light chain; Thio T, thioflavin T. A–C, G–L: scale bars = 500 µm; D–F, P–R: scale bars = 250 µm; M–O: scale bars = 100 µm.

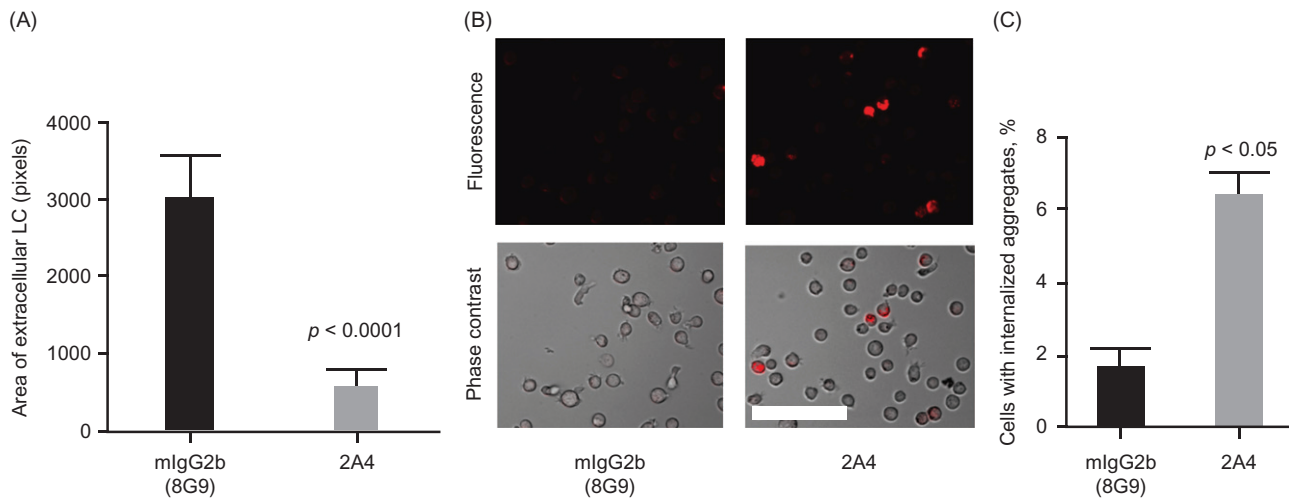

Figure 5. 2A4 promotes phagocytosis of AL amyloidosis heart extracts by a human macrophage cell line *in vitro*. (A) 2A4 promoted clearance of the extracellular AL heart deposits by THP-1 macrophages. Clearance was measured by area of extracellular LC protein deposits, immunostained for λ LC, remaining after 24 h and was significantly increased by 2A4 treatment (gray bar) compared with an isotype control antibody (black bar). Data are presented as mean ± SEM ($n = 3$). (B, C) 2A4 induced internalization of pHrodo-conjugated AL heart deposits by THP-1 cells, visualized as an increase in intracellular pHrodo-fluorescence shown in a representative bright-field overlay (20×; B) or quantified as the percentage of THP-1 cells with elevated relative mean fluorescence intensity (C), which represents internalized pHrodo-labeled aggregates. Values represent mean ± SEM of 60 optical fields per group, pooled from three independent wells (Figure 5A) or of three independent flow cytometry runs with approximately 1000 cells per run (Figure 5C). Statistical differences were determined by 2-tailed Student *t* test. Scale bar = 100 µm.

recombinant ALMC (not shown) and coupling those to pHrodo dye, we were able to directly visualize 2A4-mediated phagocytosis. This pH-sensitive fluorescent dye increases emitted fluorescence in acidic conditions, such as in the phagocytic endosomal compartment; thus, the proportion of monocytes observed with internalized fluorescence reflects the magnitude of phagocytosis. The numbers of fluorescent monocytes was substantially increased ($p < 0.05$) in cells exposed to 2A4, compared with the IgG control antibody (Figure 5B and C, Supplementary Figure S4).

Discussion

In the present study, we demonstrated that 2A4, the murine form of NEOD001, binds to an LC cryptotope that is exposed at various stages of misfolding, aggregation and fibrillization and is specific to the misfolded amyloidogenic protein. We established that 2A4 specifically binds LC in both soluble and insoluble tissue extracts from patients with AL amyloidosis. Moreover, we showed that 2A4 binds deposited LC amyloid *in situ*. We also confirmed that 2A4 can mediate the phagocytosis of LC amyloid. Together these results support the evaluation of NEOD001 in patients with AL amyloidosis. We propose that NEOD001, like 2A4, may promote the clearance of AL amyloid from affected organs and engage soluble aggregates in patients with AL amyloidosis and that it may lead to stabilization or improvement of organ function.

Increasing evidence indicates that soluble LC aggregates serve as precursors for the nucleation of amyloid deposits. In addition, soluble forms of LC may themselves be directly cytotoxic to cardiomyocytes [9–14]. In this regard, our demonstration of 2A4 binding to soluble LC aggregates from patient samples and ALMC aggregates is notable. These soluble LC intermediates may represent early stages of LC multimerization, and our results indicate that the cryptotope recognized by 2A4 is available during these initial states of protein misfolding. The apparent absence of those aggregates in many of the samples analyzed may reflect low abundance or, alternatively, that certain LC sequences are associated with faster fibrillization kinetics, thereby reducing the steady state concentrations of intermediate multimeric species in post-mortem samples.

Our results also demonstrate that the previously reported variability of 2A4 immunolabeling in tissue derived from patients with AL amyloidosis [15] likely resulted from a loss of the 2A4 epitope caused by formalin fixation of that tissue. Notably, in the present study, every patient sample tested under native, unfixed conditions was positively labeled by 2A4. Further, this positive labeling was diminished when the same sections were exposed to fixation, likely due to the effects of aldehyde cross-linking of LC, which masked the epitope. The nature of the binding specificity of 2A4 to a conformational epitope may impart a high sensitivity to the harsh chemical modifications routinely utilized in histologic studies.

Interestingly, though a predominance of either λ or κ LC amyloid was observed in most organs studied, the presence of both FLC subtypes was found in approximately one-third of patients. This has also been observed in previous studies using mass spectrometry–based proteomics [18,19,23], which suggests that, despite the clonal LC involvement in circulation, heterologous cross-seeding and aggregation might occur between involved and noninvolved LC. Cross-seeding has been proposed to affect the deposition of AL [24] and other amyloid proteins [25,26]. Although the initial nucleation and deposition of AL amyloid is typically associated with abnormal levels of clonal FLC, it is possible that further deposition of polyclonal LC may occur despite normal circulating concentrations.

One mechanism of action proposed for 2A4 and NEOD001 is the clearance of organ AL deposits that is associated with structural damage and dysfunction. 2A4 was previously shown to bind to amyloid *in vivo* and to accelerate the clearance of AL amyloidomas in association with the recruitment of immune cells [15]. The present study demonstrates that 2A4 rapidly promoted the engagement of phagocytes to engulf and clear AL deposits *in vitro*. Taken together, our results support a protein immunotherapy mechanism of action through which 2A4 promotes the clearance of AL amyloid *in vivo* by binding and opsonization of LC aggregates, followed by FcR-mediated phagocytosis and intracellular degradation by proteolytic enzymes.

An interim report from an ongoing phase 1/2 study in 27 patients with AL amyloidosis treated with NEOD001 (ClinicalTrials.gov, NCT01707264) for a median of 12 monthly infusions has recently been published [27]. NEOD001 was well tolerated, and no patient experienced infusion-related inflammatory responses. A substantial proportion of the evaluable patients demonstrated favorable renal (60%) and cardiac (57%) responses that were evident in some of them more than 2 years after their last plasma cell–directed response. The expansion phase of this study is ongoing. Two separate randomized, placebo-controlled, global trials that specifically address the safety and efficacy of NEOD001 in patients with cardiac AL amyloidosis (NCT02632786 and NCT02312206) are also ongoing.

Two antibodies in addition to NEOD001 are in clinical development for the potential treatment of patients with AL amyloidosis. One is directed against the amyloid-associated protein serum amyloid P (SAP). It is hoped the antibody will have a beneficial impact on the amyloid burden of patients with AL amyloidosis and other types of amyloid disease (e.g. AA amyloidosis, fibrinogen A alpha chain amyloidosis, apolipoprotein A-I amyloidosis) [28]. A second approach involves the anti-AL antibody 11–1F4. 11–1F4, which binds to an epitope on LC distinct from NEOD001, is a mouse–human chimeric antibody that has been reported to interfere with the hyperbolic growth phase of LC fibril formation. This antibody was originally characterized as an imaging agent, though phase 1 data in a therapeutic setting were recently reported [29].

Conclusion

The present report has demonstrated a mechanism by which 2A4 may selectively target and clear deposited amyloid. We also provide data to support that 2A4 may bind circulating LC at an early step in protein misfolding. Amyloid-directed treatments represent a significant unmet need for patients with AL amyloidosis. Although there are no approved therapies for the treatment of AL amyloidosis, plasma cell–directed therapies are often used in an attempt to control the

hematologic burden and are often associated with hematologic response. Inasmuch as hematologic response is variable and its ability to translate into organ benefit is the means by which survival is improved, it is important to consider the combination of plasma cell–directed approaches with amyloid-targeting therapies such as NEOD001; such combination treatments may lead to stabilization or improvement of organ dysfunction and may ultimately improve survival by addressing both the production of amyloidogenic LC and existing LC amyloid deposits within organs. Ongoing clinical trials addressing the safety and efficacy of NEOD001 are designed to address these possibilities.

Acknowledgements

We thank Drs Merrill Benson and Michaela Liedtke for the donated patient tissues. Atomic force microscopy measurements were performed by Michael Allen at Biometrology, Inc. (Chicago, IL). Electron microscopy imaging was performed by Jinny Wong at the Electron Microscopy Core, Gladstone Institutes (San Francisco, CA). LC-MS/MS for amyloid protein identification and LC subtyping was performed at Mayo Clinical Laboratory (Rochester, MN). Medical editorial assistance was provided by ApotheCom (San Francisco, CA).

Declaration of interest

All authors are employees of Prothena Biosciences Inc and own stock options in Prothena Biosciences Inc. This study was sponsored by Prothena Biosciences Inc, South San Francisco, CA, USA.

References

1. Merlini G, Bellotti V. Molecular mechanisms of amyloidosis. N Engl J Med 2003;349:583–96.
2. Kyle RA, Linos A, Beard CM, Linke RP, Gertz MA, O'Fallon WM, Kurland LT. Incidence and natural history of primary systemic amyloidosis in Olmsted County, Minnesota, 1950 through 1989. Blood 1992;79:1817–22.
3. Pinney JH, Smith CJ, Taube JB, Lachmann HJ, Venner CP, Gibbs SD, Dungu J, et al. Systemic amyloidosis in England: an epidemiological study. Br J Haematol 2013;161:525–32.
4. Kyle RA, Gertz MA. Primary systemic amyloidosis: clinical and laboratory features in 474 cases. Semin Hematol 1995;32:45–59.
5. Merlini G, Comenzo RL, Seldin DC, Wechalekar A, Gertz MA. Immunoglobulin light chain amyloidosis. Expert Rev Hematol 2014;7:143–56.
6. Palladini G, Hegenbart U, Milani P, Kimmich C, Foli A, Ho AD, Vidus RM, et al. A staging system for renal outcome and early markers of renal response to chemotherapy in AL amyloidosis. Blood 2014;124:2325–32.
7. Merlini G, Wechalekar AD, Palladini G. Systemic light chain amyloidosis: an update for treating physicians. Blood 2013;121:5124–30.
8. Gertz MA, Comenzo R, Falk RH, Fermand JP, Hazenberg BP, Hawkins PN, Merlini G, et al. Definition of organ involvement and treatment response in immunoglobulin light chain amyloidosis (AL): a consensus opinion from the 10th International Symposium on Amyloid and Amyloidosis, Tours, France, 18–22 April 2004. Am J Hematol 2005;79:319–28.
9. Brenner DA, Jain M, Pimentel DR, Wang B, Connors LH, Skinner M, Apstein CS, et al. Human amyloidogenic light chains directly impair cardiomyocyte function through an increase in cellular oxidant stress. Circ Res 2004;94:1008–10.
10. Guan J, Mishra S, Shi J, Plovie E, Qiu Y, Cao X, Gianni D, et al. Stanniocalcin1 is a key mediator of amyloidogenic light chain induced cardiotoxicity. Basic Res Cardiol 2013;108:378.
11. Lavatelli F, Imperlini E, Orrù S, Rognoni P, Sarnataro D, Palladini G, Malpasso G, et al. Novel mitochondrial protein interactors of immunoglobulin light chains causing heart amyloidosis. Faseb J 2015;29:4614–28.
12. McWilliams-Koeppen HP, Foster JS, Hackenbrack N, Ramirez-Alvarado M, Donohoe D, Williams A, Macy S, et al. Light chain amyloid fibrils cause metabolic dysfunction in human cardiomyocytes. PLoS One 2015;10:e0137716.
13. Shi J, Guan J, Jiang B, Brenner DA, del Monte F, Ward JE, Connors LH, et al. Amyloidogenic light chains induce cardiomyocyte contractile dysfunction and apoptosis via a non-canonical p38alpha MAPK pathway. Proc Natl Acad Sci USA 2010;107:4188–93.
14. Liao R, Jain M, Teller P, Connors LH, Ngoy S, Skinner M, Falk RH, et al. Infusion of light chains from patients with cardiac amyloidosis causes diastolic dysfunction in isolated mouse hearts. Circulation 2001;104:1594–7.
15. Wall JS, Kennel SJ, Williams A, Richey T, Stuckey A, Huang Y, Macy S, et al. AL amyloid imaging and therapy with a monoclonal antibody to a cryptic epitope on amyloid fibrils. PLoS One 2012;7:e52686.
16. Arendt BK, Ramirez-Alvarado M, Sikkink LA, Keats JJ, Ahmann GJ, Dispenzieri A, Fonseca R, et al. Biologic and genetic characterization of the novel amyloidogenic lambda light chain-secreting human cell lines, ALMC-1 and ALMC-2. Blood 2008;112:1931–41.
17. Puchtler H, Sweat F, Levine M. On the binding of Congo red by amyloid. J Histochem Cytochem 1962;10:355–64.
18. Vrana JA, Gamez JD, Madden BJ, Theis JD, Bergen HR III, Dogan A. Classification of amyloidosis by laser microdissection and mass spectrometry-based proteomic analysis in clinical biopsy specimens. Blood 2009;114:4957–9.
19. Rodriguez FJ, Gamez JD, Vrana JA, Theis JD, Giannini C, Scheithauer BW, Parisi JE, et al. Immunoglobulin derived depositions in the nervous system: novel mass spectrometry application for protein characterization in formalin-fixed tissues. Lab Invest 2008;88:1024–37.
20. Cohen AS, Calkins E. The isolation of amyloid fibrils and a study of the effect of collagenase and hyaluronidase. J Cell Biol 1964;21:481–6.
21. Dapson RW. Macromolecular changes caused by formalin fixation and antigen retrieval. Biotech Histochem 2007;82:133–40.
22. Pepys MB, Booth DR, Hutchinson WL, Gallimore JR, Collins PM, Hohenester E. Amyloid P component. A critical review. Amyloid 1997;4:274–95.
23. Mollee P, Renaut P, Boros S, Loo D, Hill M. Diagnosis of amyloidosis subtype by laser-capture microdissection (LCM) and tandem mass spectrometry (MS/MS) proteomic analysis. Blood 2013;122:5295.
24. Blancas-Mejia LM, Ramirez-Alvarado M. Recruitment of light chains by homologous and heterologous fibrils shows distinctive kinetic and conformational specificity. Biochemistry 2016;55:2967–78.
25. Oskarsson ME, Paulsson JF, Schultz SW, Ingelsson M, Westermark P, Westermark GT. In vivo seeding and cross-seeding of localized amyloidosis: a molecular link between type 2 diabetes and Alzheimer disease. Am J Pathol 2015;185:834–46.
26. Morales R, Moreno-Gonzalez I, Soto C. Cross-seeding of misfolded proteins: implications for etiology and pathogenesis of protein misfolding diseases. PLoS Pathogens 2013;9:e1003537.
27. Gertz MA, Landau H, Comenzo RL, Seldin DC, Weiss B, Zonder J, Merlini G, et al. First-in-human phase I/II study of NEOD001 in patients with light chain amyloidosis and persistent organ dysfunction. J Clin Oncol 2016;34:1097–103.
28. Richards DB, Cookson LM, Berges AC, Barton SV, Lane T, Ritter JM, Fontana M, et al. Therapeutic clearance of amyloid by antibodies to serum amyloid P component. N Engl J Med 2015;373:1106–14.
29. Langer A, Miao S, Mapara M, Radhakrishnan J, Maurer MS, Raza S, Mears JG, et al. Results of phase I study of chimeric fibril-reactive monoclonal antibody 11-1F4 in patients with AL amyloidosis. Presented at: 57th American Society of Hematology Annual Meeting; December 5-8, 2015; Orlando, Florida. Abstract 188.

Supplementary material available online
Supplementary Figures S1–S4